Inorg. Chem. **2004**, *43*, 4825–4832

Inorganic Chemistry Article

Synthesis, Structural, Spectroscopic, and Electrochemical Characterization of High Oxidation State Diruthenium Complexes Containing Four Identical Unsymmetrical Bridging Ligands

Karl M. Kadish,*,† Tuan D. Phan,† Li-Lun Wang,† Lingamallu Giribabu,† Antoine Thuriere,† Julien Wellhoff,† Shurong Huang,† Eric Van Caemelbecke,†,‡ and John L. Bear*,†

Department of Chemistry, University of Houston, Houston, Texas 77204-5003, and
Department of Chemistry, Houston Baptist University, Texas 77074-3298

Received January 8, 2004

Six Ru_2^{6+} derivatives of the form $Ru_2(L)_4(C{\equiv}CC_6H_5)_2$, where L = 2-Fap, 2,3-$F_2$ap, 2,4-$F_2$ap, 2,5-$F_2$ap, 3,4-$F_2$ap, or 2,4,6-$F_3$ap, are synthesized and characterized as to their electrochemical, spectroscopic, and/or structural properties. These compounds are synthesized from a reaction between $LiC{\equiv}CC_6H_5$ and $Ru_2(L)_4Cl$. Two of the investigated complexes exist in a (4,0) isomeric form while four adopt a (3,1) geometric conformation. These two series of geometric isomers are compared with previously characterized (4,0) $Ru_2(ap)_4(C{\equiv}CC_6H_5)_2$, (4,0) $Ru_2(F_5ap)_4(C{\equiv}CC_6H_5)_2$, and (3,1) $Ru_2(F_5ap)_4(C{\equiv}CC_6H_5)_2$. The overall data on the nine compounds thus provide an opportunity to systematically examine how the electrochemical and structural properties of these Ru_2^{6+} complexes vary with respect to isomer type and electronic properties of the bridging ligands.

Introduction

A large number of diruthenium complexes coordinated by equatorial and axial ligands containing substantially different σ and π donor/acceptor properties have been synthesized and characterized as to their spectroscopic and electrochemical properties.[1−25] Among these compounds are a group of substituted anilinopyridine bridged complexes of the type $Ru_2(L)_4Cl$, where L is one of the eight anionic ligands shown in Chart 1. These complexes can also exist in up to four different isomeric forms, (4,0), (3,1), (2,2)-cis, or (2,2)-trans, depending upon the number and position of fluorine atoms on the phenyl group of the anilinopyridinate anion, but in virtually all cases, only one or two isomers are detected for a given compound. These are the (4,0) and (3,1) isomers.[9,26−29]

---

* Author to whom correspondence should be addressed. E-mail: kkadish@uh.edu.

† University of Houston.

‡ Houston Baptist University.

(1) Chakravarty, A. R.; Cotton, F. A. *Inorg. Chim. Acta* **1986**, *113*, 19.
(2) Malinski, T.; Chang, D.; Feldmann, F. N.; Bear, J. L.; Kadish, K. M. *Inorg. Chem.* **1983**, *22*, 3225.
(3) Chakravarty, A. R.; Cotton, F. A. *Polyhedron* **1985**, *4*, 1957.
(4) Miskowski, V. M.; Loehr, T. M.; Gray, H. B. *Inorg. Chem.* **1987**, *26*, 1098.
(5) Lindsay, A. J.; Wilkinson, G.; Motevalli, M.; Hursthouse, M. B. *J. Chem. Soc., Dalton Trans.* **1987**, *2723*.
(6) Cotton, F. A.; Ren, T. *Inorg. Chem.* **1991**, *30*, 3675.
(7) Cotton, F. A.; Matusz, M. *J. Am. Chem. Soc.* **1988**, *110*, 5761.
(8) Das, B. K.; Chakravarty, A. R. *Inorg. Chem.* **1990**, *29*, 2078.
(9) Bear, J. L.; Li, Y.; Han, B.; Van Caemelbecke, E.; Kadish, K. M. *Inorg. Chem.* **1997**, *36*, 5449.
(10) Ren, T. *Coord. Chem. Rev.* **1998**, *175*, 43.
(11) Bear, J. L.; Han, B.; Huang, S. *J. Am. Chem. Soc.* **1993**, *115*, 1175.
(12) Bear, J. L.; Li, Y.; Han, B.; Van Caemelbecke, E.; Kadish, K. M. *Inorg. Chem.* **1996**, *35*, 3053.
(13) Bear, J. L.; Han, B.; Huang, S.; Kadish, K. M. *Inorg. Chem.* **1996**, *35*, 3012.
(14) Bear, J. L.; Li, Y.; Han, B.; Kadish, K. M. *Inorg. Chem.* **1996**, *35*, 1395.
(15) Lin, C.; Ren, T.; Valente, E. J.; Zubkowski, J. D. *J. Chem. Soc., Dalton Trans.* **1998**, 571.
(16) Bear, J. L.; Li, Y.; Cui, J.; Han, B.; Van Caemelbecke, E.; Phan, T.; Kadish, K. M. *Inorg. Chem.* **2000**, *39*, 857.
(17) Bear, J. L.; Li, Y.; Han, B.; Van Caemelbecke, E.; Kadish, K. M. *Inorg. Chem.* **2001**, *40*, 182.
(18) Bear, J. L.; Chen, W.-Z.; Han, B.; Huang, S.; Wang, L.-L.; Thuriere, A.; Van Caemelbecke, E.; Kadish, K. M.; Ren, T. *Inorg. Chem.* **2003**, *42*, 6230.
(19) Cotton, F. A.; Walton, R. A. *Multiple Bonds Between Metal Atoms*; Oxford University Press: Oxford, 1993.
(20) Xu, G.; Ren, T. *Organometallics* **2001**, *20*, 2400.
(21) Ren, T. *Organometallics* **2002**, *21*, 732.
(22) Hurst, S. K.; Ren, T. *J. Organomet. Chem.* **2003**, *670*, 188.
(23) Hurst, S. K.; Xu, G.-L.; Ren, T. *Organometallics* **2003**, *22*, 4118.
(24) Xu, G.; Ren, T. *J. Organomet. Chem.* **2002**, *655*, 239.
(25) Xu, G.-L.; DeRosa, M. C.; Crutchley, R. J.; Ren, T. *J. Am. Chem. Soc.* **2004**, *126*, 3728.
(26) Chakravarty, A. R.; Cotton, F. A.; Tocher, D. A. *Inorg. Chem.* **1985**, *24*, 172.
(27) Bear, J. L.; Wellhoff, J.; Royal, G.; Van Caemelbecke, E.; Eapen, S.; Kadish, K. M. *Inorg. Chem.* **2001**, *40*, 2282.
(28) Kadish, K. M.; Wang, L.-L.; Thuriere, A.; Van Caemelbecke, E.; Bear, J. L. *Inorg. Chem.* **2003**, *42*, 834.

10.1021/ic0499594 CCC: $27.50 © 2004 American Chemical Society

Published on Web 07/10/2004

Chart 1

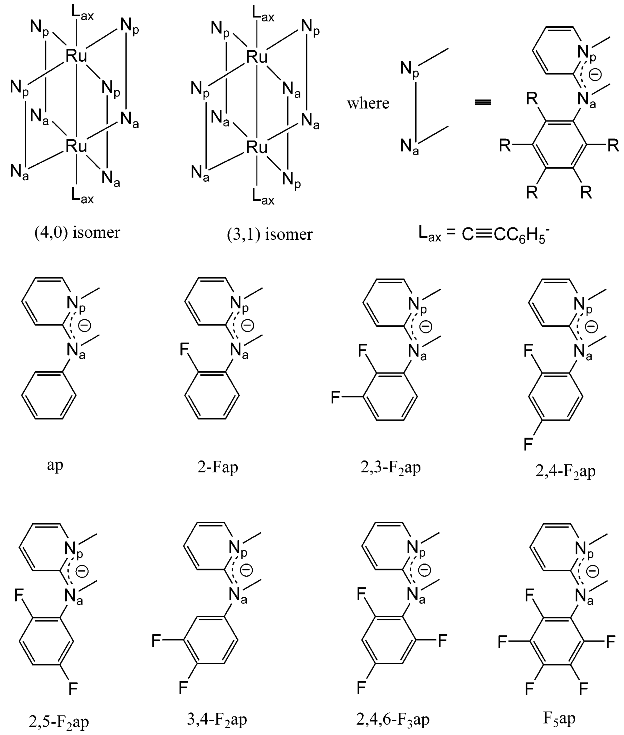

Most Ru_2^{5+} complexes of this type can undergo two metal-centered oxidations and one metal-centered reduction under a N_2 atmosphere,[28] giving compounds with Ru_2^{6+}, Ru_2^{7+}, and Ru_2^{4+} cores. However, under a CO atmosphere,[29] five oxidation states may be electrogenerated for the same series of compounds. These are Ru_2^{6+}, Ru_2^{5+}, Ru_2^{4+}, Ru_2^{3+}, and Ru_2^{2+}.

Linear free energy relationships and isomer effects on the structural and electrochemical properties of low oxidation state anilinopyridinate (ap) and substituted ap complexes have both been reported,[28,29] and it was of interest to examine high oxidation state compounds with the same type of bridging ligands and the same isomer type. This is described in the current Article, which builds upon earlier reported structural and electrochemical results for other related compounds which have four identical unsymmetrical bridging ligands.[9,24]

Six new Ru_2^{6+} derivatives of the form $Ru_2(L)_4(C{\equiv}CC_6H_5)_2$, where L = 2-Fap, 2,3-F$_2$ap, 2,4-F$_2$ap, 2,5-F$_2$ap, 3,4-F$_2$ap, or 2,4,6-F$_3$ap, are synthesized and characterized in the present Article as to their electrochemical, spectroscopic, and/or structural properties. The data on these six complexes are then compared with previously characterized (4,0) $Ru_2(ap)_4(C{\equiv}CC_6H_5)_2$, (4,0) $Ru_2(F_5ap)_4(C{\equiv}CC_6H_5)_2$, and (3,1) $Ru_2(F_5ap)_4(C{\equiv}CC_6H_5)_2$. Four of the nine compounds exist in a (4,0) isomeric form while five adopt a (3,1) geometric conformation. These two series of compounds thus provide a large enough number of derivatives to examine how the electrochemical and structural properties of these Ru_2^{6+} complexes vary with respect to isomer type and electronic properties of the bridging ligands. As will be shown, the Ru_2^{7+}, Ru_2^{5+}, and Ru_2^{4+} forms of the compounds are all stable on the cyclic voltammetry time scale, and the measured $E_{1/2}$ values are discussed in terms of the electronic properties of the bridging ligands and the isomer type, (4,0) or (3,1). These data are also compared to results obtained in parallel studies carried out on $Ru_2(dpf)_4(C{\equiv}CC_6H_5)_2$ and its derivatives, where dpf is the *N,N′*-diphenylformamidinate anion.

$Ru_2(dpf)_4(C{\equiv}C)_x$ (x = 2 or 4) has been used as a precursor[30] for the synthesis of nanomolecular assemblies with the aim of generating conducting polymers as well as nonlinear optical systems, and one can anticipate that both the electronic effect of the bridging ligands and the arrangement of the bridging ligands around the dimetal core, i.e., (4,0) or (3,1), may alter the conducting and/or nonlinear optical properties of synthesized molecules that contain a $Ru_2(L)_4(C{\equiv}C)_x$ unit where L is ap or a substituted ap bridging ligand.

Experimental Section

Chemicals and Reagents. High-purity nitrogen was purchased from Matheson-Trigas Co. and was passed through anhydrous calcium sulfate and potassium hydroxide pellets to remove trace oxygen and water prior to use. GR grade dichloromethane, *n*-hexane (Aldrich), absolute dichloromethane (Fluka) for electrochemical measurements, and absolute ethyl alcohol (McCormick, Inc.) for recrystallization were used without purification. Lithium phenylacetylide ($LiC{\equiv}CC_6H_5$) in 0.1 M THF was purchased from Aldrich and used as received. Tetra-*n*-butylammonium perchlorate (TBAP) was purchased from Fluka Chemical Co., twice recrystallized from ethyl alcohol, and stored in a vacuum oven at 40 °C for at least one week prior to use. Silica gel (Merck 230−400 mesh 60 Å) and anhydrous THF were all purchased from Aldrich and used as received.

Physical Measurements. Cyclic voltammetry was carried out using either an EG&G Princeton applied research (PAR) model 173 or a 263 potentiostat/galvanostat. A three-electrode system was used and consisted of a glassy carbon working electrode, a platinum wire counter electrode, and a homemade saturated calomel electrode (SCE) as the reference electrode. The SCE was separated from the bulk of the solution by a fritted-glass bridge of low porosity that contained the solvent/supporting electrolyte mixture. All potentials are referenced to the SCE, and all measurements were carried out at room temperature.

UV−visible spectra were recorded with a Hewlett-Packard model 8453 diode array spectrophotometer. IR spectra were recorded on a FTIR Nicolet 550 Magna-IR spectrophotometer. Elemental analyses were carried out by Atlantic Microlab, Inc., Norcross, GA. Mass spectra were recorded either on a Finnigan TSQ 700 instrument at the University of Texas, Austin or on an Applied Biosystem Voyager DE-STR MALDI-TOF mass spectrometer equipped with a nitrogen laser (337 nm) at the University of Houston Mass Spectrometry Laboratory.

Synthesis of Starting Materials. The three (4,0) isomers of $Ru_2(L)_4Cl$ (L = ap, 2,5-F$_2$ap, or 3,4-F$_2$ap), the four (3,1) isomers of $Ru_2(L)_4Cl$ (L = 2-Fap, 2,3-F$_2$ap, 2,4-F$_2$ap, or 2,4,6-F$_3$ap) as well as (4,0) $Ru_2(ap)_4(C{\equiv}CC_6H_5)_2$ were prepared as described in the literature.[24,26−29]

---

(29) Kadish, K. M.; Phan, T.; Giribabu, L.; Shao, J.; Wang, L.-L.; Thuriere, A.; Van Caemelbecke, E.; Bear, J. L. *Inorg. Chem.* **2004**, *43*, 1012.

(30) Wong, K.-T.; Lehn, J.-M.; Peng, S.-M.; Lee, G.-H. *Chem. Commun.* **2000**, 2259.

Synthesis of $Ru_2(L)_4(C{\equiv}CC_6H_5)_2$ Complexes. $Ru_2(L)_4(C{\equiv}CC_6H_5)_2$ (L = 2-Fap, 2,3-F_2ap, 2,4-F_2ap, 2,5-F_2ap, 3,4-F_2ap, or 2,4,6-F_3ap) was synthesized by stirring a mixture of $Ru_2(L)_4Cl$ and $Li(C{\equiv}CC_6H_5)$ in deaerated THF in a 1:25 molar ratio under N_2 for 10 h. During this time, the color gradually changed from dark green to dark red. Upon exposure to air, the color of the solution changed to dark blue within 30 min. Evaporation of the solvent yielded in each case a dark blue residue, which was purified by silica gel column chromatography using a mixture of CH_2Cl_2/*n*-hexane (3/7, v/v) to give $Ru_2(L)_4(C{\equiv}CC_6H_5)_2$.

(4,0) $Ru_2(3,4\text{-}F_2ap)_4(C{\equiv}CC_6H_5)_2$ (1). Yield: 60%. Mass spectral data [*m*/*e*, (fragment)]: 1228 $[Ru_2(3,4\text{-}F_2ap)_4(C{\equiv}CC_6H_5)_2]^+$, 1126 $[Ru_2(3,4\text{-}F_2ap)_4(C{\equiv}CC_6H_5)]^+$, 1022 $[Ru_2(3,4\text{-}F_2ap)_4]^+$. Anal. Calcd for $C_{60}H_{38}N_8F_8Ru_2$: C, 63.82; H, 3.09; N, 9.93. Found: C, 63.72; H, 3.04; N, 9.91. IR (cm^{-1}): 2080 [$\nu(C{\equiv}C)$]. UV−vis spectrum in CH_2Cl_2 [λ_{max}, nm ($\epsilon \times 10^{-3}$, M^{-1} cm^{-1})]: 623 (5.9), 1031 (2.0).

(4,0) $Ru_2(2,5\text{-}F_2ap)_4(C{\equiv}CC_6H_5)_2$ (2). Yield: 35%. Mass spectral data [*m*/*e*, (fragment)]: 1228 $[Ru_2(2,5\text{-}F_2ap)_4(C{\equiv}CC_6H_5)_2]^+$, 1126 $[Ru_2(2,5\text{-}F_2ap)_4(C{\equiv}CC_6H_5)]^+$, 1022 $[Ru_2(2,5\text{-}F_2ap)_4]^+$. Anal. Calcd for $C_{60}H_{38}N_8F_8Ru_2$: C, 63.82; H, 3.09; N, 9.93. Found: C, 63.74; H, 3.02; N, 9.88. IR (cm^{-1}): 2081 [$\nu(C{\equiv}C)$]. UV−vis spectrum in CH_2Cl_2 [λ_{max}, nm ($\epsilon \times 10^{-3}$, M^{-1} cm^{-1})]: 622 (6.4), 1030 (1.8).

(3,1) $Ru_2(2\text{-}Fap)_4(C{\equiv}CC_6H_5)_2$ (3). Yield: 58%. Mass spectral data [*m*/*e*, (fragment)]: 1154 $[Ru_2(2\text{-}Fap)_4(C{\equiv}CC_6H_5)_2]^+$, 1053 $[Ru_2(2\text{-}Fap)_4(C{\equiv}CC_6H_5)]^+$, 952 $[Ru_2(2\text{-}Fap)_4]^+$. IR (cm^{-1}): 2084 [$\nu(C{\equiv}C)$]. UV−vis spectrum in CH_2Cl_2 [λ_{max}, nm ($\epsilon \times 10^{-3}$, M^{-1} cm^{-1})]: 369 (4.9), 615 (3.2).

(3,1) $Ru_2(2,4\text{-}F_2ap)_4(C{\equiv}CC_6H_5)_2$ (4). Yield: 69%. Mass spectral data [*m*/*e*, (fragment)]: 1228 $[Ru_2(2,4\text{-}F_2ap)_4(C{\equiv}CC_6H_5)_2]^+$, 1126 $[Ru_2(2,4\text{-}F_2ap)_4(C{\equiv}CC_6H_5)]^+$, 1022 $[Ru_2(2,4\text{-}F_2ap)_4]^+$. Anal. Calcd for $C_{60}H_{38}N_8F_8Ru_2$: C, 63.82; H, 3.09; N, 9.93. Found: C, 63.91; H, 3.10; N, 9.90. IR (cm^{-1}): 2081 [$\nu(C{\equiv}C)$]. UV−vis spectrum in CH_2Cl_2 [λ_{max}, nm ($\epsilon \times 10^{-3}$, M^{-1} cm^{-1})]: 455 (4.0), 627 (3.1).

(3,1) $Ru_2(2,4,6\text{-}F_3ap)_4(C{\equiv}CC_6H_5)_2$ (5). Yield: 52%. Mass spectral data [*m*/*e*, (fragment)]: 1296 $[Ru_2(2,4,6\text{-}F_3ap)_4(C{\equiv}CC_6H_5)_2]^+$, 1195 $[Ru_2(2,4,6\text{-}F_3ap)_4(C{\equiv}CC_6H_5)]^+$, 1094 $[Ru_2(2,4,6\text{-}F_3ap)_4]^+$. IR ($cm^{-1}$): 2080 [$\nu(C{\equiv}C)$]. UV−vis spectrum in CH_2Cl_2 [λ_{max}, nm ($\epsilon \times 10^{-3}$, M^{-1} cm^{-1})]: 466 (8.1), 634 (12.3), 892 (3.1).

(3,1) $Ru_2(2,3\text{-}F_2ap)_4(C{\equiv}CC_6H_5)_2$ (6). Yield: 68%. Mass spectral data [*m*/*e*, (fragment)]: 1228 $[Ru_2(2,3\text{-}F_2ap)_4(C{\equiv}CC_6H_5)_2]^+$, 1126 $[Ru_2(2,3\text{-}F_2ap)_4(C{\equiv}CC_6H_5)]^+$, 1022 $[Ru_2(2,3\text{-}F_2ap)_4]^+$. Anal. Calcd for $C_{60}H_{38}N_8F_8Ru_2$: C, 63.82; H, 3.09; N, 9.93. Found: C, 63.99; H, 3.15; N, 9.87. IR (cm^{-1}): 2079 [$\nu(C{\equiv}C)$]. UV−vis spectrum in CH_2Cl_2 [λ_{max}, nm ($\epsilon \times 10^{-3}$, M^{-1} cm^{-1})]: 450 (3.8), 630 (2.8)

X-ray Crystallography of Compounds 3 and 5. Single-crystal X-ray crystallographic studies were performed at the University of Houston X-ray Crystallographic Center. Each sample was placed in a steam of dry nitrogen gas at −50 °C in a random position. The radiation used was Mo Kα monochromatized by a highly ordered graphite crystal. Final cell constants as well as other information pertinent to data collection and structure refinement are listed in Table 1.

The measurement for **3** was made with a Nicolet R3m/V automatic diffractometer, while the measurement for **5** was made with a Siemens SMART platform diffractometer equipped with a 1K CCD area detector. A hemisphere of data 1271 frames at 5 cm detector distance was collected using a narrow-frame method with scan widths of 0.30° in ω and an exposure time of 35 s/frame (**3**) or 25 s/frame (**5**). The first 50 frames were remeasured at the end of data collection to monitor instrument and crystal stability, and the maximum correction on *I* was <1%. The data were integrated using the Siemens SAINT program, with the intensities corrected for Lorentz factor, polarization, air absorption, and absorption because of variation in the path length through the detector faceplate. A Ψ-scan absorption correction was applied on the basis of the entire data set. Redundant reflections were averaged. Final cell constants were refined using 4332 reflections for **3** and 6241 reflections for **5** having $I > 10\sigma(I)$. The Laue symmetries were determined to be $\bar{1}$ for compound **3** and 2/*m* for compound **5**, and from the systematic absences noted, the space groups were shown to be $P\bar{1}$ for **3** and $P2_{1/c}$ for **5**.

Table 1. Crystal Data and Data Collection and Processing Parameters for the (3,1) Isomers of **3** and **5**

	$Ru_2(2\text{-}Fap)_4(C{\equiv}CC_6H_5)_2$ (**3**)	$Ru_2(F_3ap)_4(C{\equiv}CC_6H_5)_2$ (**5**)
space group	$P\bar{1}$ triclinic	$P2_{1/c}$ monoclinic
cell constant		
a (Å)	12.0286(7)	11.0146(5)
b (Å)	14.4427(9)	19.7799(9)
c (Å)	17.7049(11)	24.1941(11)
α (deg)	110.649(1)	90.00
β (deg)	97.758(1)	101.145(1)
γ (deg)	103.353(1)	90.00
V (Å^3)	2720.1(3)	5171.7(4)
mol formula	$C_{60}H_{42}N_8F_4Ru_2.CH_2Cl_2$	$C_{60}H_{34}N_8F_{12}Ru_2$
fw (g/mol)	1238.08	1297.09
Z	2	4
ρ_{calcd} (g/cm^3)	1.512	1.666
μ (cm^{-1})	0.715	0.678
λ (Mo Kα) (Å)	0.71073	0.71073
temp (K)	223	223
R (F_o)[a]	0.0457	0.0235
R_w (F_o)[b]	0.1297	0.0126

[a] $R = \Sigma|F_o| - |F_c|/\Sigma|F_o|$. [b] $R_w = [\Sigma_w(|F_o| - |F_c|)^2/\Sigma_w|F_o|^2]^{1/2}$.

Results and Discussion

Synthesis and Reaction Mechanism for Compounds 1−6. The air-stable Ru_2^{6+} complexes, formulated as $Ru_2(L)_4(C{\equiv}CC_6H_5)_2$ (L = 2-Fap, 2,3-F_2ap, 2,4-F_2ap, 2,5-F_2ap, 3,4-F_2ap, or 2,4,6-F_3ap), were synthesized and characterized with respect to their electrochemical and/or structural properties. The exact stoichiometry of the reaction depends on the amount of added $LiC{\equiv}CC_6H_5$, and the bis-adduct $Ru_2(L)_4(C{\equiv}CC_6H_5)_2$ is favored over the monoadduct $Ru_2(L)_4(C{\equiv}CC_6H_5)$ when a large excess of $LiC{\equiv}CC_6H_5$ is used.[9,11] Therefore, a large excess of $LiC{\equiv}CC_6H_5$ (25 mmol) was reacted with $Ru_2(L)_4Cl$ (1 mmol) to maximize the yield of $Ru_2(L)_4(C{\equiv}CC_6H_5)_2$. The sequence of reactions shown in eqs 1−3 has been proposed for the synthesis of $Ru_2(L)_4(C{\equiv}CC_6H_5)_2$ (L = dpf, ap, or F_5ap),[9,15,24] and these three reactions can also account for synthesis of the $Ru_2(L)_4(C{\equiv}CC_6H_5)_2$ derivatives examined in the present study.

$$Ru_2(L)_4Cl + C{\equiv}CC_6H_5^- \rightarrow Ru_2(L)_4(C{\equiv}CC_6H_5) + Cl^- \quad (1)$$

$$Ru_2(L)_4(C{\equiv}CC_6H_5) + C{\equiv}CC_6H_5^- \rightarrow Ru_2(L)_4(C{\equiv}CC_6H_5)_2^- \quad (2)$$

$$Ru_2(L)_4(C{\equiv}CC_6H_5)_2^- + \text{air} \rightarrow Ru_2(L)_4(C{\equiv}CC_6H_5)_2 \quad (3)$$

Equation 1 involves the replacement of the Cl^- anion by one phenylacetylide anion, and this reaction is followed by the addition of a second phenylacetylide ion in a trans arrangement as shown in eq 2. The air-stable Ru_2^{6+} complex, $Ru_2(L)_4(C{\equiv}CC_6H_5)_2$, is then obtained by air oxidation of the

Table 2. Selected Average Bond Lengths (Å) and Bond Angles (deg) for the (4,0) and (3,1) Isomers of $Ru_2(L)_4(C{\equiv}CC_6H_5)_2$

	(4,0) isomer		(3,1) isomer		
L	ap[a]	F_5ap[b]	2-Fap (**3**)	2,4,6-F_3ap (**5**)	F_5ap[b]
			Bond Lengths (Å)		
Ru−Ru	2.4707(8)	2.441(1)	2.4689(6)	2.4640(2)	2.475(1)
$Ru-N_a$	2.050	2.072	2.020	2.034	2.075
$Ru-N_p$	2.067	2.065	2.130	2.101	2.050
Ru−C	1.988	1.953	2.002	1.984	1.983
C−C	1.203	1.211	1.203	1.206	1.214
			Bond Angles (deg)		
Ru−Ru−C	163.4	171.4	161.0	164.3	163.2
$Ru-Ru-N_a$	85.60	87.65	90.31	88.31	90.48
$Ru-Ru-N_p$	87.00	85.91	83.08	85.78	84.21
N−Ru−Ru−N	22.40	20.40	18.20	17.90	14.40

[a] Taken from ref 24. [b] Taken from ref 9.

a) (3,1) $Ru_2(2\text{-Fap})_4(C{\equiv}CC_6H_5)_2$ (**3**)

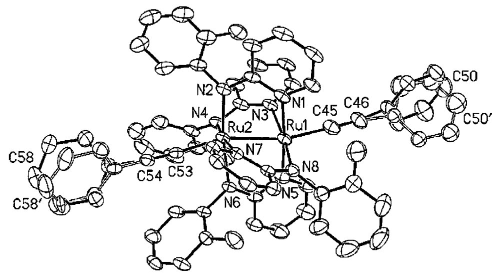

b) (3,1) $Ru_2(2,4,6\text{-}F_3ap)_4(C{\equiv}CC_6H_5)_2$ (**5**)

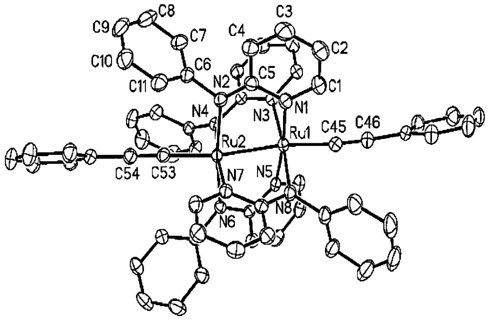

Figure 1. Molecular structures for the (3,1) isomer of (a) $Ru_2(2\text{-Fap})_4(C{\equiv}CC_6H_5)_2$ (**3**) and (b) $Ru_2(2,4,6\text{-}F_3ap)_4(C{\equiv}CC_6H_5)_2$ (**5**). H and/or F atoms have been omitted for clarity.

Ru_2^{5+} species as shown in eq 3. The last step in this mechanism is consistent with the fact that in each case the solution turns from red to blue upon exposing the solution to air (see Experimental Section).

The final bis-ligated Ru_2^{6+} product was purified by silica gel column chromatography and obtained in yields ranging from 52 to 69%; no increase in the yield was observed when the mixture was left to react for a longer time.

Molecular Structures of Compounds 3 and 5. Selected average bond lengths and average bond angles for compounds **3** and **5** are summarized in Table 2, along with data for (4,0) $Ru_2(ap)_4(C{\equiv}CC_6H_5)_2$, (4,0) $Ru_2(F_5ap)_4(C{\equiv}CC_6H_5)_2$, and (3,1) $Ru_2(F_5ap)_4(C{\equiv}CC_6H_5)_2$. The molecular structures of compounds **3** and **5** are illustrated in Figure 1a,b, respectively. All intramolecular bond lengths and bond angles as well as other structural data of the two compounds are given in the Supporting Information. The coordination of each Ru atom is essentially octahedral with four "substituted ap" bridging ligands forming the equatorial plane. For compounds **3** and **5**, Ru1 is coordinated to an axial phenylacetylide group and to three pyridyl nitrogen atoms and one anilino nitrogen atom, while Ru2 is coordinated to three anilino nitrogen atoms, one pyridyl nitrogen atom, and an axial phenylacetylide ligand.

The Ru−Ru bond lengths of **3** and **5** are 2.469(6) Å and 2.464(2) Å, respectively. These values are comparable to those of the ap[24] and the two F_5ap[9] complexes and are within the range of 2.316−2.599 Å for Ru−Ru bond distances of other reported Ru_2^{6+} compounds of the type $Ru_2(L)_4(X)_2$, where L = DiMeODMBA (*N*,*N*′-dimethyl-3,5-dimethoxybenzamidinate) or DmAniF (di-*m*-methoxyphenylformamidinate) and X = Cl^- or $(C{\equiv}C)_2Si(CH_3)_3^-$.[31,32] As shown in Table 2, there is no obvious correlation between the substituent effect of the bridging ligand and the bond lengths or bond angles in the (3,1) isomers of $Ru_2(L)_4(C{\equiv}CC_6H_5)_2$. For example, the Ru−Ru−C bond angle increases from 161.0° to 164.3° upon going from L = 2-Fap to 2,4,6-F_3ap but decreases from 164.3° to 163.2° upon going from 2,4,6-F_3ap to F_5ap. The $Ru_2(L)_4$ framework is less distorted when it has more electron-withdrawing groups on the bridging ligands as shown by the fact that, in the (4,0) isomer series, the average N−Ru−Ru−N torsion angle follows the order: ap (22.40°) > F_5ap (20.40°) while in the (3,1) isomer series it follows the order: 2-Fap (18.20°) > 2,4,6-F_3ap (17.90°) > F_5ap (14.40°). One might have predicted an opposite relationship if the steric hindrance between the axial and bridging ligands is proposed to account for the twist of the structural frame.

The Ru−Ru bond distances of Ru_2^{6+} complexes bridged by ap and substituted ap ligands are significantly shorter than the Ru−Ru bond distances of Ru_2^{6+} compounds with dpf or substituted dpf ligands, and this can be attributed to the features of the ap ligand itself since the N−C−N angle of the ap ligand is smaller than that of the dpf ligand (see Chart 2). A similar trend was also observed in the case of Ru_2^{5+} complexes with ap or dpf ligands.[13,28] The Ru−Ru bond lengths in $Ru_2(L)_4(C{\equiv}CC_6H_5)_2$ (L = ap, 2-Fap, 2,4,6-F_3ap, or F_5ap) are, however, comparable to those of $Ru_2[((m\text{-MeO})\text{DMBA})_4(C{\equiv}CC_6H_5)_2$ (2.447(9) Å) and $Ru_2(DEBA)_4(C{\equiv}CC_6H_5)_2$ (2.458(9) Å) (where ((*m*-MeO)DMBA) is *N*,*N*′-

---

(31) Xu, G.-L.; Jablonski, C. G.; Ren, T. *J. Organomet. Chem.* **2003**, *683*, 388.

(32) Xu, G.; Ren, T. *Inorg. Chem.* **2001**, *40*, 2925−2927.

Chart 2

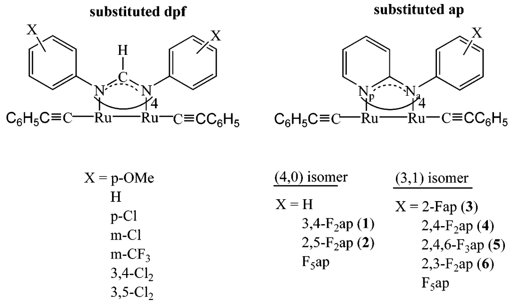

Table 3. Comparison of Ru−Ru Bond Lengths (Å) of the (4,0) and (3,1) Isomers of $Ru_2(L)_4Cl$ and $Ru_2(L)_4(C{\equiv}CC_6H_5)_2$ Complexes, Where L Is ap or a Substituted ap Ligand

		bond length (Å)	
isomer type	ligand, L	$Ru_2(L)_4Cl$	$Ru_2(L)_4(C{\equiv}CC_6H_5)_2$
(4,0)	ap	2.275(3)	2.470(3)
(3,1)	2-Fap	2.286(3)	2.469(6)
	2,4,6-F$_3$ap	2.284(6)	2.464(2)

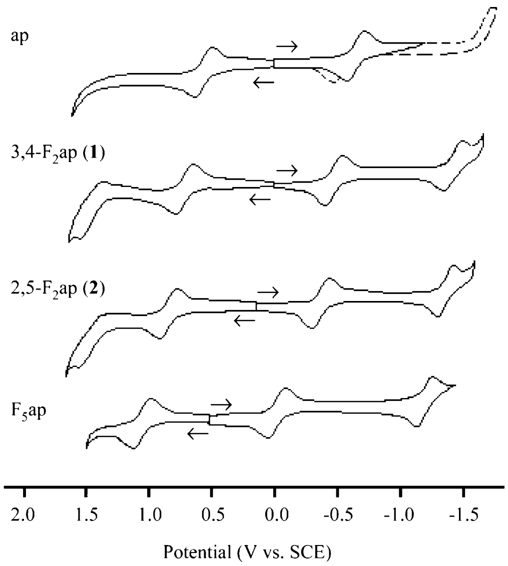

Figure 2. Cyclic voltammograms of (4,0) $Ru_2(L)_4(C{\equiv}CC_6H_5)_2$ (L = ap, 3,4-F$_2$ap, 2,5-F$_2$ap or F$_5$ap) in CH_2Cl_2 containing 0.1 M TBAP. Scan rate = 0.1 V/s. Dashed line shows current−voltage curve obtained upon scanning the potential beyond the second reduction of the compound.

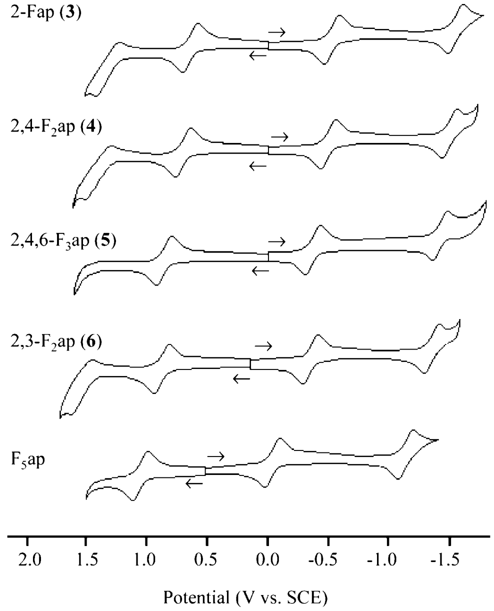

Figure 3. Cyclic voltammograms of (3,1) $Ru_2(L)_4(C{\equiv}CC_6H_5)_2$ (L = 2-Fap, 2,4-F$_2$ap, 2,3-F$_2$ap, 2,4,6-F$_3$ap or F$_5$ap) in CH_2Cl_2 containing 0.1 M TBAP. Scan rate = 0.1 V/s.

dimethyl-*m*-methoxybenzamidinate and DEBA is *N,N′*-dialkylbenzamidinate).[23,31]

The nature of the axial ligand L in $Ru_2(ap)_4(L)$ complexes is known to affect the Ru−Ru bond length. For example, $Ru_2(ap)_4(C{\equiv}CR)$ has a Ru−Ru bond length of 2.362(5) Å when R = $Si(CH_3)_3$ and 2.3234(7) Å when R = CH_2OCH_3.[33] Both values are slightly larger than in $Ru_2(ap)_4Cl$, a compound with a Ru−Ru bond length of 2.275(3) Å, thus showing a slight elongation of the Ru−Ru bond upon going from L = Cl^- to L = $C{\equiv}CR^-$. A slight increase in the Ru−Ru bond distance is also observed upon changing the oxidation state from Ru_2^{5+} to Ru_2^{6+}. For example, the Ru−Ru bond length of $Ru_2(ap)_4Cl$ is 0.03 Å shorter than that in $[Ru_2(ap)_4Cl]^+$.[34] However, neither the change in oxidation state from Ru_2^{5+} to Ru_2^{6+} nor the change in the type of axial ligand from Cl^- to $C{\equiv}CR^-$ can account for the large increase of 0.018−0.195 Å seen upon going from $Ru_2(L)_4Cl$ to $Ru_2(L)_4(C{\equiv}CC_6H_5)_2$, where L = ap, 2-Fap, or 2,4,6-F$_3$ap (see Table 3). This elongation of the Ru−Ru bond has been explained for the case of L = ap in terms of a change in the electronic configuration from $\sigma^2\pi^4\delta^2\pi^{*2}\delta^*$ for the five-coordinate complex to $\pi^4\delta^2\pi^{*4}$ for the six-coordinate acetylide derivative with two $C{\equiv}CC_6H_5^-$ ligands on the diruthenium core.[24]

A similar conclusion can be proposed to rationalize the elongation of the Ru−Ru bond in the case of the 2-Fap and 2,4,6-F$_3$ap derivatives. This result is also consistent with the fact that these two compounds, as well as all other investigated $Ru_2(L)_4(C{\equiv}CC_6H_5)_2$ complexes, have active NMR spectra, which is expected if these diruthenium derivatives all possess the electronic configuration $\pi^4\delta^2\pi^*$.[4]

Electrochemistry of $Ru_2(L)_4(C{\equiv}CC_6H_5)_2$. The redox behavior of (4,0) $Ru_2(ap)_4(C{\equiv}CC_6H_5)_2$ and compounds **1**−**6** was investigated by cyclic voltammetry in the noncoordinating solvent CH_2Cl_2 containing 0.1 M TBAP, and the data were compared to the (4,0) and (3,1) isomers of $Ru_2(F_5ap)_4(C{\equiv}CC_6H_5)_2$.[9] Cyclic voltammograms of (4,0) $Ru_2(ap)_4(C{\equiv}CC_6H_5)_2$, (4,0) $Ru_2(F_5ap)_4(C{\equiv}CC_6H_5)_2$, **1** and **2** are shown in Figure 2, while cyclic voltammograms of compounds **3**−**6** are illustrated in Figure 3 along with (3,1) $Ru_2(F_5ap)_4(C{\equiv}CC_6H_5)_2$. Half-wave potentials of the investigated complexes are listed in Table 4 along with half-wave potentials for the (4,0) and (3,1) isomers of $Ru_2(F_5ap)_4(C{\equiv}CC_6H_5)_2$.

Five of the nine electrochemically examined Ru_2^{6+} complexes (**1**−**4** and **6**) undergo four one-electron metal-centered processes (two oxidations and two reductions), while for the ap derivative, the two isomers of F$_5$ap, and compound **5**, only three metal-centered processes are seen, one of which is an oxidation and the others are reductions. A stepwise

---

(33) Zou, G.; Alvarez, J. C.; Ren, T. *J. Organomet. Chem.* **2000**, *596*, 152.
(34) Cotton, F. A.; Yokochi, A. *Inorg. Chem.* **1997**, *36*, 567.

Table 4. Half-Wave Potentials (V vs SCE) in CH_2Cl_2 Containing 0.1 M TBAP and UV−Vis Spectral Data of $Ru_2(L)_4(C{\equiv}CC_6H_5)_2$ in CH_2Cl_2

		redox reactions				λ_{max}, nm ($\epsilon \times 10^{-3}$, M^{-1} cm^{-1})				
$\Sigma\sigma^a$	ligand, L	$Ru_2^{8+/7+}$	$Ru_2^{7+/6+}$	$Ru_2^{6+/5+}$	$Ru_2^{5+/4+}$	band I	band II	band III	$\epsilon_{I/II}$	$\epsilon_{II/II}$
				(4,0) Isomer						
0.00	ap		0.55	−0.54	-1.67^b	452(6.9)	633(5.6)	1011(3.0)	1.23	1.87
0.40	3,4-F_2ap (**1**)	1.42	0.70	−0.45	−1.45		623(5.9)	1031(2.8)		2.11
0.58	2,5-F_2ap (**2**)	1.43	0.76	−0.42	−1.39		629(6.4)	1030(3.4)		1.85
1.22	F_5ap		0.90	−0.05	−1.18	450	650		1.13	
				(3,1) Isomer						
0.24	2-Fap (**3**)	1.31	0.62	−0.58	−1.54	469(4.9)	615(3.2)		1.53	
0.30	2,4-F_2ap (**4**)	1.38	0.70	−0.56	−1.50	455(4.0)	627(3.1)		1.30	
0.54	2,4,6-F_3ap (**5**)		0.78	−0.42	−1.47	466(2.0)	634(3.1)	892(0.8)	0.64	3.90
0.58	2,3-F_2ap (**6**)	1.50	0.80	−0.40	−1.40	450(3.8)	630(2.8)		1.40	
1.22	F_5ap		1.00	−0.13	−1.15	480	650	1055	0.62	4.00

[a] Taken from ref 34. [b] E_{pc} value.

conversion between compounds with Ru_2^{7+}, Ru_2^{6+}, Ru_2^{5+}, or Ru_2^{4+} cores can therefore be electrochemically accomplished as shown by eqs 4−6 for all of the investigated compounds, while Ru_2^{8+} can be seen only for compounds **1**−**4** and **6** (eq 7). The ap, F_5ap derivatives, and **5** cannot be converted to a Ru_2^{8+} oxidation state under our utilized experimental conditions. The notation for the compound is given below as $(L)_4Ru_2^{n+}$ where n = 4, 5, 6, 7, or 8.

$$(L)_4Ru_2^{6+} + e^- \rightleftarrows (L)_4Ru_2^{5+} \tag{4}$$

$$(L)_4Ru_2^{5+} + e^- \rightleftarrows (L)_4Ru_2^{4+} \tag{5}$$

$$(L)_4Ru_2^{6+} \rightleftarrows (L)_4Ru_2^{7+} + e^- \tag{6}$$

$$(L)_4Ru_2^{7+} \rightleftarrows (L)_4Ru_2^{8+} + e^- \tag{7}$$

Plots of $E_{1/2}$ vs the sum of substituent constants ($\Sigma\sigma$)[35] for the three redox reactions given by eqs 4−6 of both (4,0) and (3,1) isomers of $Ru_2(L)_4(C{\equiv}CC_6H_5)_2$ are shown in Figure 4a,b, respectively. The dependence of $E_{1/2}$ on the electronic effect of the substituents can be quantified by linear least-squares fit of the data to the Hammett relationship as shown in eq 8:[36,37]

$$\Delta E_{1/2} = E_{1/2}(X) - E_{1/2}(H) = 4\Sigma\sigma\rho \tag{8}$$

where ρ is the reactivity constant. Because there are four equivalent bridging ligands on each investigated Ru_2^{6+} complex, $4\Sigma\sigma$ is used in eq 8. The reactivity constants (ρ) and the correlation coefficients (R) for the plots in Figure 4 are listed in Table 5 along with the values of the substituted dpf complexes with the same two $C{\equiv}CC_6H_5^-$ axial ligands.[15] The good correlation coefficient (R) values in Table 5 indicate that the same electron-transfer mechanism occurs for each redox process in the two series of isomers.

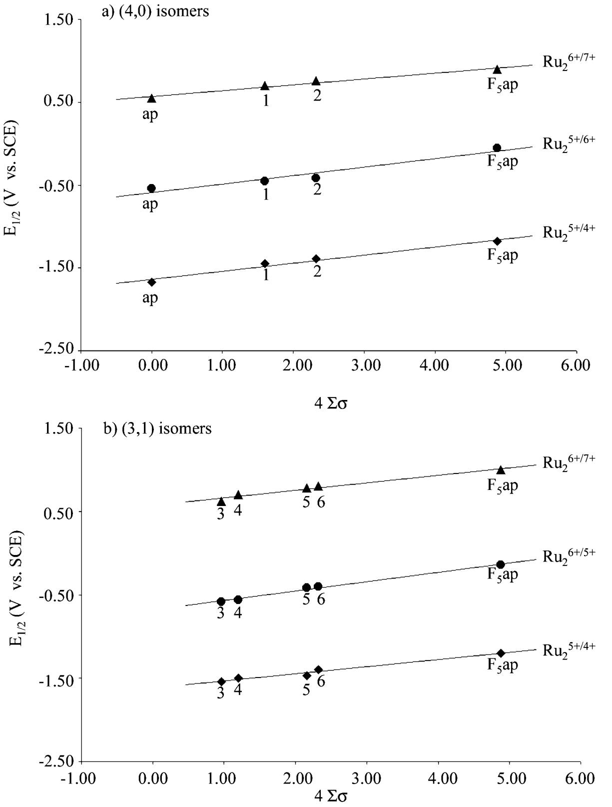

Figure 4. Linear free energy relationships for the redox reactions of (a) (4,0) isomers and (b) (3,1) isomers of $Ru_2(L)_4(C{\equiv}CC_2H_5)_2$.

Table 5. Comparison of ρ Values (mV) for the (4,0) and (3,1) Isomers of Ru_2(ap-type)$_4(C{\equiv}CC_6H_5)_2$ and Ru_2(dpf-type)$_4(C{\equiv}CC_6H_5)_2$, with R Values of Linear-Square Fit Given in Parentheses

	redox reaction		
compounds	$Ru_2^{5+/4+}$	$Ru_2^{6+/5+}$	$Ru_2^{7+/6+}$
(4,0) isomers	98 (0.98)	102 (0.94)	70 (0.98)
(3,1) isomers	85 (0.97)	112 (0.99)	90 (0.97)
substituted dpf[a]	81 (0.99)	92 (0.99)	72 (0.99)

[a] Taken from ref 15.

As shown in Table 5, the ρ values of $Ru_2(L)_4(C{\equiv}CC_6H_5)_2$ range from 70 to 112 mV. The exact value depends on the redox couple in both series of isomers, but different trends are seen for the (4,0) and (3,1) isomers. For the (4,0) isomers, the ρ values of the $Ru_2^{5+/4+}$ and $Ru_2^{6+/5+}$ redox couples are of similar magnitude and both are larger than the ρ value for the $Ru_2^{7+/6+}$ process, while for the (3,1) isomers, the ρ value of the $Ru_2^{6+/5+}$ redox couple is larger than that of the $Ru_2^{5+/4+}$ and $Ru_2^{7+/6+}$ processes.

The ρ value for the $Ru_2^{7+/6+}$ and $Ru_2^{6+/5+}$ redox couples also increases upon going from the (4,0) to (3,1) isomers while the ρ value of the $Ru_2^{5+/4+}$ process shows an opposite

---

(35) Zuman, P. *Substituent Effects in Organic Polarography*; Plenum Press: New York, 1967.

(36) Zuman, P. *The Elucidation of Organic Electrode Process*; Academic Press: London, 1967.

(37) Hammett, L. P. *Physical Organic Chemistry*; Wiley: New York, 1970.

trend (see Table 5), thus suggesting that the substituent effect of the bridging ligands also varies with the isomer type. This is also the case for the parent Ru_2^{5+} complexes.[28]

The ρ values for a given redox process of the substituted ap and substituted dpf complexes in Chart 2 depend on the symmetry of the bridging ligands, i.e., symmetrical vs unsymmetrical as shown by comparing the ρ values of $Ru_2^{n+/(n-1)+}$ for Ru_2^{6+} complexes bridged by substituted ap ligands to those of Ru_2^{6+} complexes containing substituted dpf bridging ligands (see Table 5). Overall, the data in Table 5 suggest that the substituted ap complexes usually exhibit a greater substituent effect than the substituted dpf derivatives, and a similar conclusion was also reached in the case of Ru_2^{5+} complexes with the same bridging ligands (ap or dpf).[28]

The proposed electronic configuration $\pi^4\delta^2\pi^{*4}$ of all $Ru_2(L)_4(C{\equiv}CC_6H_5)_2$ derivatives implies that the reduction of each compound involves the addition of an electron to the first available antibonding δ^* orbital, while the oxidation involves the removal of an electron from the π^* orbital. As discussed above, only the first oxidation of the compounds differs significantly in the ρ values upon going from the (4,0) to (3,1) isomers, thus suggesting that the substituent effect on the energy level of the π^* orbital is more sensitive to the isomer type than the substituent effect on the energy level of the δ^* orbital.

UV−Vis Studies. The UV−vis absorption features of the investigated compounds are given in Table 4, and the UV−vis spectra of the (4,0) and (3,1) isomers of $Ru_2(L)_4(C{\equiv}CC_6H_5)_2$ are given in the Supporting Information Figures S1 and S2, respectively. The number of absorption bands depends on both the type of isomer and the type of bridging ligands. For instance, in the case of (4,0) isomer, the 3,4-F_2ap and 2,5-F_2ap complexes exhibit bands II and III while the F_5ap derivative shows bands I and II and the ap derivative shows all three bands (I, II, and III). The ratio of ϵ values between bands I and II, $\epsilon_{I/II}$, is 1.23 for the ap derivative, and this is similar to a value of 1.13 for the $\epsilon_{I/II}$ of the F_5ap derivative. The $\epsilon_{II/III}$ values of the 3,4-F_2ap and 2,5-F_2ap are also virtually the same, but they differ from the $\epsilon_{II/III}$ value of the ap complex.

Somewhat similar relationships are also seen for compounds having a (3,1) conformation, as shown in Table 4. All of the (3,1) isomeric complexes exhibit bands I and II with the exception of the F_3ap and F_5ap derivatives, which exhibit an extra band III of weak intensity. However, the ratio of molar absorptivities between bands I and II of the (3,1) isomeric complexes possessing four redox reactions differs from those of the (3,1) isomeric compounds that exhibit only three redox reactions. For example, the values of $\epsilon_{I/II}$ for the 2-Fap, 2,4-F_2ap, and 2,3-F_2ap complexes range from 1.30 to 1.53, while the values of $\epsilon_{I/II}$ for the F_3ap and F_5ap derivatives are 0.64 and 0.62, respectively.

Similar UV−vis spectral changes are observed upon oxidation of (4,0) $Ru_2(3,4\text{-}F_2ap)_4(C{\equiv}CC_6H_5)_2$ and (3,1) $Ru_2(F_3ap)_4(C{\equiv}CC_6H_5)_2$, although the (4,0) isomer undergoes two oxidations while the (3,1) isomer undergoes only one (Figure 5). The spectral data and the electrochemical results are therefore self-consistent, and both suggest that each Ru_2^{7+} species has the electronic configuration of $\pi^4\delta^2\pi^{*3}$ independent of the isomer type and number of oxidations seen by cyclic voltammetry. One may therefore wonder why a formal $Ru_2^{8+/7+}$ process is observed for compounds **1**−**4** and **6** but not for the other investigated compounds. The electronic configuration of the Ru_2^{7+} species indicates that the second oxidation will involve the removal of one electron from a π^* orbital. It has been reported that the two π^* orbitals can have different energy levels,[38] thus suggesting that the removal of one electron from the lower energy π^* orbital is more difficult to access, and this could explain why the ap, F_3ap, and F_5ap complexes undergo only one oxidation. However, further theoretical studies will be needed to confirm this interpretation of the data.

a) (4,0) $Ru_2(3,4\text{-}F_2ap)_4(C{\equiv}CC_6H_5)_2$, 1st oxidation at 1.0 V

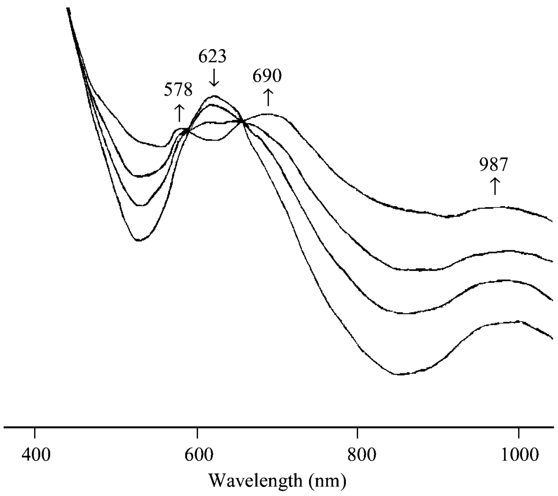

b) (3,1) $Ru_2(F_3ap)_4(C{\equiv}CC_6H_5)_2$, 1st oxidation at 1.2 V

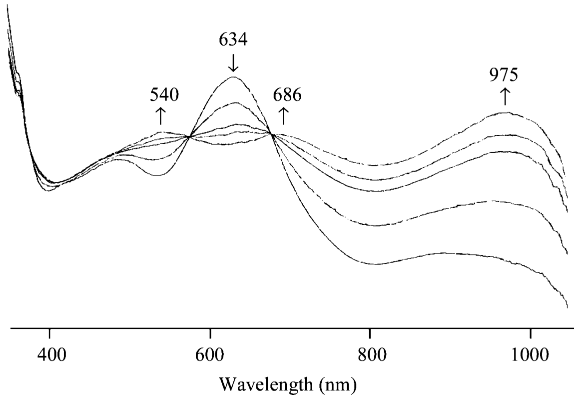

Figure 5. Thin-layer UV−visible spectral changes of (a) (4,0) $Ru_2(3,4\text{-}F_2ap)_4(C{\equiv}CC_6H_5)_2$ and (b) (3,1) $Ru_2(F_3ap)_4(C{\equiv}CC_6H_5)_2$ in CH_2Cl_2, 0.2 M TBAP upon the first oxidation.

Summary

Six Ru_2^{6+} complexes of the type $Ru_2(L)_4(C{\equiv}CC_6H_5)_2$, which exist in (3,1) or (4,0) isomeric form, were examined as to their electrochemical, spectroscopic, and/or structural properties. The structural data suggest that the $Ru_2(L)_4$ framework is not significantly affected by the bridging ligand

---

(38) Wesemann, J. L.; Chisholm, M. H. *Inorg. Chem.* **1997**, *36*, 3258.

or the isomer type; a similar trend was observed for the Ru_2^{5+} derivatives with ap or substituted ap bridging ligands. As is the case for the ap derivative, the Ru_2^{6+} complexes with two $C{\equiv}CC_6H_5^-$ axial ligands have much longer Ru−Ru bond distances than their parent Ru_2^{5+} compounds. All of the investigated complexes undergo two one-electron reductions and one or two one-electron oxidations. The first oxidation and both reductions follow linear free energy relationships between $E_{1/2}$ and the Hammett parameter of the substituents on the bridging ligands.

Acknowledgment. The support of the Robert A. Welch Foundation (J.L.B., Grant E-918; K.M.K., Grant E-680) is gratefully acknowledged. We thank Dr. J. D. Korp for performing the X-ray analysis.

Supporting Information Available: X-ray crystallographic files in CIF format for structural determination of (3,1) $Ru_2(2\text{-}Fap)_4(C{\equiv}CC_6H_5)_2$ (**4**) and (3,1) $Ru_2(2,4,6\text{-}F_3ap)_4(C{\equiv}CC_6H_5)_2$ (**6**). UV−visible spectra of investigated complexes are given in Figure S1 (4,0 isomer) and Figure S2 (3,1 isomer). This material is available free of charge via the Internet at http://pubs.acs.org.

IC0499594